A Proposal for Silicon Detectors with high Position and Timing Resolution as Roman Pots at EIC

Roman Pots @ EIC

EIC Detector R&D Proposal May 2019

Project ID:
Project Name: Si-RP@EIC
Period Reported: FY19 (New Proposal)
Project Leader: A. Tricoli & E.C. Aschenauer
Contact Person: A. Tricoli & E.C. Aschenauer

Project Members

A.Tricoli
BNL ATLAS Group
E.C. Aschenauer, A. Jentsch
BNL ME Group
S. Fazio, A. Kiselev
BNL STAR HI Group
G. Giacomini
BNL Instrumentation Group
C. Da Via
Stony Brook University

Content:

1. Answers to the Proposal Evaluation

To accurately determine Generalized Parton Distributions (GPDs) and Transverse Momentum Dependent parton distributions (TMDs), that enable a study of the spatial distribution of quarks and gluons inside the proton or nucleons, measurements of exclusive reactions is required. This requirement of exclusivity demands that all final state products are detected. Instrumented Roman Pots with fast timing detectors in the far forward region will increase the coverage for exclusive measurements and can help in the background rejection. The development and fabrication at BNL of edgeless AC-coupled 4D silicon detectors based on the LGAD design to instrument the Roman Pots is proposed. The performance of these sensors will be compared with the performance of active edge 3D silicon sensors. At the end of the first year the physics performance goals for Roman Pots at the EIC will be articulated, the detector requirements for detectors in Roman Pots at the EIC will be specific and three batches of AC-LGADs will be fabricated and their performance compared to 3D silicon sensors. The effort is highly leveraged with ongoing activities at Brookhaven. A total support at the level of $35k is requested.

1.1. Evaluation:

Instrumented Roman Pots will enhance the capability for exclusive measurements. However, why a timing resolution of 10 picoseconds is required is not articulated in the proposal. For a flight path of 40 meters and a proton momentum of 50 GeV, the dt/dm is about 50ps/GeV. A good timing resolution would indeed provide a new constraint for tracking and momentum, but this ambitious goal of 10 picoseconds has not been motivated in the proposal.

As discussed in section 1.5 of the proposal the goal is to resolve event-by-event a collision occurred at the head or the tail of the proton bunch. For eRHIC the RMS of the proton bunch length is predicted to vary from 13 cm to 7 cm depending on the hadron beam energy and accelerator configuration. The lepton bunch length is around 1 cm for the different lepton beam energies and configurations.

Figure 1 shows that after the transverse momentum kick $p_x(z)$ from the crab cavity to the particle bunch, with the kicking strength proportional to the longitudinal position z of particles in the bunch. The intensity profile of a bunch is after the crabbing identical to the one in an accelerator without crossing angle, but the particle momentum vector gets an additional component in x, which has the same effect on the smearing of the scattering angle of diffractive protons as an increased angular divergence.

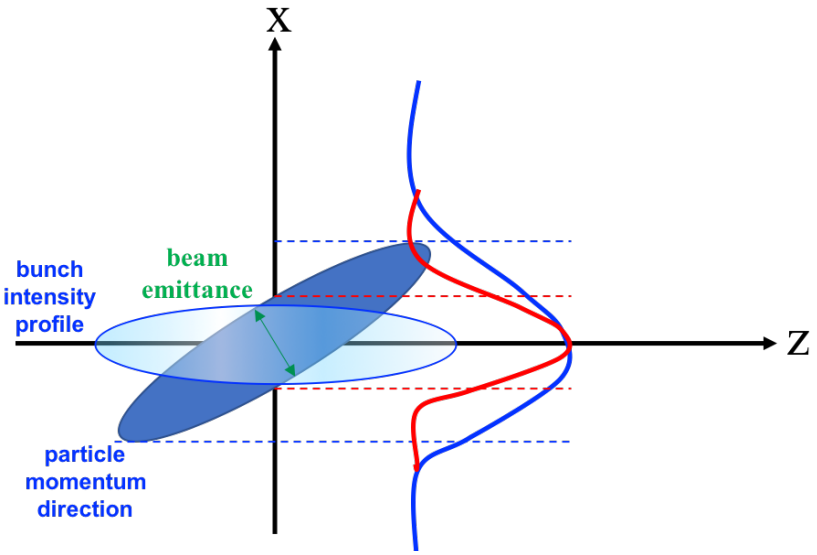

Figure 1: Schematic representation of the intensity profile of the ions in a bunch (light blue ellipse) and the momentum direction (dark blue ellipse) of the ions in the bunch after the crab cavity. Note the transverse and longitudinal size of the bunches much more elongated as shown here (100 μm vs 10 cm).

We have performed two simulations to study the effect on the p_t-resolution of diffractively scattered protons as measured by the Roman Pots corresponding to a beam without crab crossing effects and one with the maximum effect, the results are presented in Table 1 and Figure 2. The simulation result without the effect of the crab cavities uses beam parameters and optics information corresponding to the high divergence optics of eRHIC without strong hadron cooling for the center of mass energy with the highest luminosity (see

Table 2). This is the optics planned to be used if the running of eRHIC focusses on diffractive measurements, in electron-proton collisions. For both simulations the Roman Pots consist of two Silicon detector planes. The first one placed at 35 m from the IP with a distance between them of 2 m. This setup is very similar to what is currently used successfully in RHIC. The thickness of each Silicon detector plane is 300 µm.

It is noted that all the simulations presented in the EIC-WP and references in their used a p_T resolution for the protons reconstructed in the Roman Pots of 5 MeV and a systematic uncertainty of 5% on the cross section. These assumptions have been guided by the HERA experience. The ZEUS leading proton spectrometer equipped with silicon microstrips detectors used for the DVCS $d\sigma/d|t|$ measurement, achieved a p_T - resolution of 5 MeV [ZEUS Collaboration, S. Chekanov et al. , JHEP 0905 , 108 (2009).].

Therefore to unfold the smearing of the p_t-resolution due to the bunch rotation because of the crab cavities requires a precise determination of the vertex and with a timing resolution of the Silicon detectors of the Roman Pots in the order of 20 ps this should be possible. The exact requirements for timing resolution and pixel size are part of the deliverable of this proposal.

	Beam Spot (x,y)	Theta (mrad)	Phi (degree)	Pixel Size (x,y)	p_T resolution
No crabbing	100µm x20µm	0 - 4	0 - 90	55µm x 55µm	3.3 MeV/c
With crabbing	1 mm x 20 µm	0 - 4	0 - 90	55µm x 55µm	16 Mev /c

Table 1: Simulation results to show the significant worthening of the p_t-resolution of diffractive protons detected in the Roman Pots.

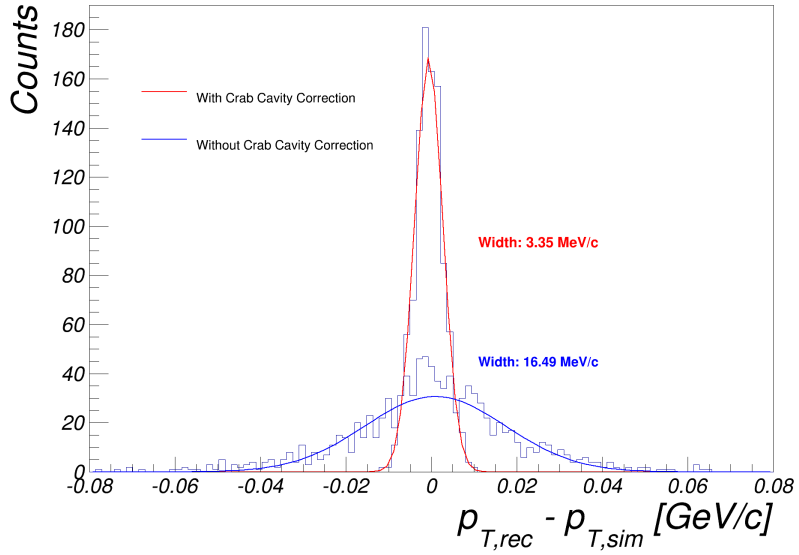

Figure 2: p_t resolution of the diffractively scattered protons as measured by the Roman pots for the 2 discussed simulation setups.

PARAMETERS	Proton	Electron
energy, GeV	275	10
relativistic factor	293.1	19569.5
bunch_intensity,E10	9.789	22.02
number_of_bunches	290	
beam_current,A	0.36	0.8
rms_normaliz._emittance,h/v_um	5.9/2.50	391/96.6
rms_emittance,h/v_nm	20.3/8.5	20.0/4.9
emittance_y/emittance_x	0.421	0.247
beta,h/v_cm	90/5.9	91/10.2
IP_beam_size,h/v_um	135/22.4	135/22.4
K=sgm_y/sgm_x	0.166	
IP_rms_ang_spread,h/v_urad	150/380	148/220
beam-beam_parameter,h/v	0.008/0.003	0.096/0.065
long._bunch_area,evs	0.8	
rms_bunch_length,cm	9.9	0.83
rms_energy_spread,e-4	4.7	5.8
max_space_charge	0.001	neglig.
Piwinski_angle,rad	8.1	1.6
Longit._IBS_time,h	8	
Transv._IBS_time,h	18.61	
lumi_factor	0.81	
luminosity,E33	**1.05**	

Table 2: eRHIC parameters for the high divergence optics without strong hadron cooling.

The proponents are kindly requested to explain why existing solutions that have been implemented in the CMS-Totem Precision Proton Spectrometer, for example, and the ongoing efforts on active edge sensors, is not adequate for the EIC.

Other forward physics detectors, e.g. the CMS-Totem Precision Proton Spectrometer (CT-PPS) and the ATLAS Forward Proton detector (AFP) at the LHC, have set similar targets for time resolution, in the range 10-30 ps, and spatial resolution of about 10-30 µm, and have been confronted with similar problematics as those under study in this proposal for EIC. However, these detectors have different constraints due to the different accelerator environments, most importantly the CT-PPS and AFP technologies have to cope with high level of radiation and pileup, which are not major concerns at EIC.

As an example for such technologies, the CT-PPS collaboration evaluated several technologies, including those proposed here for EIC, i.e. 3D detectors and LGADs. The CT-PPS is equipped with diamond detectors as timing detectors that complement the tracking silicon strip detectors. In its final configuration, the CT–PPS will use 3D silicon pixel sensors for tracking, which is deemed to provide the best performance in terms of active region and radiation hardness, and diamond sensors for timing, which are among the most radiation hard technologies on the market. During the R&D phase the CT-PPS collaboration also considered using 3D sensors for timing measurements.

On the other hand, ATLAS AFP design is not easily applicable to the EIC context due to the different space constrains at EIC compared to LHC. For EIC one can place the RPs only at a z location where the +/- 4 mrad cone from forward going neutrons is spatially separated from the scattered protons. This gives according to Figure 12 only very limited space in z. Separating the timing and tracking planes one will need more longitudinal space to fit all tracking layers for the two stations as well as the timing layers. The evaluation of a compact solution, similar to the AFP design and based on 3D sensors and separate timing detectors, for EIC is integral part of the studies in this project for requirement setting for the Roman Pots at EIC.

Other fast-time technologies, such as Cherenkov-based e.g. quartz or gaseous, can be viable options but are not considered in this proposal, where we aim to reach fine segmentation. Diamond-based technologies for application at EIC will be an expensive solution and the radiation hardness properties of diamond detectors will be unnecessary in the EIC environment.

The ultra-fast silicon technologies at the time of the CT-PPS TDR were not advanced enough to guarantee fast-timing in a high radiation environment. In the past years the R&D on ultra-fast silicon technologies, and more specifically on LGADs, has made significant progress, and now this technology is considered reliable for HL-LHC applications. At the time of the CT-PPS construction the LGADs technologies had yet unresolved challenges, e.g. intrinsic detector resolution, resistance to radiation, and the development of suitable low noise and fast electronics. These challenges have been solved by ATLAS and CMS experiments for the HL-LHC, and the LGAD technology is now mature: LGAD can be made very thin (30-50 microns) with high gain, low noise and adequately fast electronics have been developed. In addition, the novel design of a fine granularity, pixelated LGAD, i.e, AC-LGAD, that BNL is pursuing is a game changer, as it allows to combine in a single detector both tracking and timing capabilities, that so far have been implemented in separate detectors. In addition to reduced costs, this technology will also ensure low occupancy per pixel and make possible to stack several detectors to improve the time resolution using several layers. The AC-coupling technology in AC-LGADs , thanks to a continuous gain layer that covers the entire sensor area, also allows high geometrical signal collection efficiency over the whole sensor area.

AFP: http://atlas-project-lumi-fphys.web.cern.ch/atlas-project-lumi-fphys/AFP/default.html
CT-PPS: https://cds.cern.ch/record/1753795

Many of the references are rather old and the proponents are encouraged to look at more recent results that have been obtained within the AIDA program, for example, on the development of active edge sensors.

A recent work about Active Edge silicon pixel sensors is the following:
G. Calderini et al. ”Active-edge FBK-INFN-LPNHE thin n-on-p pixel sensors for the upgrade of the ATLAS Inner Tracker,” NIM A, Volume 936, 21 August 2019, Pages 638-639, https://doi.org/10.1016/j.nima.2018.10.035

A 4-pad AC-LGAD device is estimated to have a time resolution of the order of few tens of ps. This result is on a par with devices that have been fabricated already. How is the design going to be modified to obtain a 10ps timing resolution?

LGADs with time resolution better than a few tens of picoseconds must be fabricated on thinner substrates. Nowadays, the standard thickness of the silicon layer on which LGADs are fabricated is 50 um: going to 30-35 um will decrease the Landau fluctuations and hence improve the timing performance. The drawback of this approach is that the signal generated in the thinner bulk will be lower. This can be compensated for by a larger gain. For an improved timing resolution, the implantation parameters (dose and energy) of the gain layer will be adjusted. Since AC-LGADs are fabricated on the same silicon substrate and with same gain as standard LGADs, they will feature similar timing performance. The design of the AC-LGAD will not change dramatically, but the parameters of ion implantations must be tuned to account for the new substrates: gain layer and the resistive *n*-layer must be tuned accordingly. It is under consideration the possibility to also use a different thickness of the dielectrics between the AC-coupled metal pads (electrodes) and the resistive *n*-layer.

Clarification is also requested regarding system aspects. For example, provide estimates for power consumption per pixel and/or per cm^2?

The AC-LGADs fabricated by BNL show a leakage current before irradiation of about 1 nA/cm^2 at an operating voltage of about 200, for a power consumption of about 0.2 microA/cm^2, which is comparable to the leakage current in standard LGAD sensors fabricated by Hamamatsu. Post-irradiation studies of LGADs show an increase in power dissipation to about than 10 microA/cm^2 at -30 °C at a fluence of 10^{13} 1 MeV neutron equivalent / cm^2, based on studies with sensors by Hamamatsu. At high fluences, the sensors are typically operated

at low temperatures (e.g. -30 °C), but in the case of EIC, where the max fluence per year is expected to be in the order of 10^{11} 1 MeV neutron equivalent / cm^2, operating the sensors at –30 °C is not deemed necessary. The neutron flux was measured during 2017 in the IR of the STAR detector at forward rapidities close to the beam pipe ($\eta \sim 4$), no significant dependence on the luminosity was observed. The proton bunch current during the 2017 RHIC 500 GeV pp running was 1.1 10^{11} which is comparable to eRHIC (max 2 10^{11} protons / per bunch).

Power consumption in the final detector will be dominated by front-end electronics, however the RPs will not be installed in a dense environment, differently from vertex tracker, thus power consumption is less of a concern. However, power dissipation of the electronics is beyond the scope of this proposal that focuses on technology R&D and prototyping.

Also, what is time measured with respect to - we note that a one-degree change in the temperature of a 10 m cable is about a 5 ps change in electrical length and typical collider bunches are many tens of ps long?

For the time calibration we will leverage the expertise of the ATLAS and CMS timing detectors teams with whom BNL is in close collaboration. For such many-channel detectors of several m^2 of silicon, the precise time calibration is of paramount importance and challenging, whereas Roman Pots in this proposal will ultimately cover a smaller area one plane consist of 2 Si-detector in a L-shape form with the 2 longest sides to be 40 cm x 20 cm, and the cable length can be set to be the same for all channels to minimize differences in signal delays and temperature. We will also study the technique implemented in the CMS CT-PPS Roman Pot detector for achieving sub-picosecond time synchronization of the detector stations located at approximately ±220 m from the LHC interaction region in CMS. This experiment uses a master/slave synchronization concept with a single electronics module placed in each arm that is synchronized via an RF feedback system, operating at a frequency of about 480 MHz, over a single coaxial cable. This technique has the benefit of automatically compensating for the phase drift from any temperature-induced changes in the cable length.

The time is measured with respect to a common reference time (t0). The challenge of combining measurements with picosecond range precision for signals generated in locations separated by large distances requires a very precise and stable clock distribution. However, for the case of Roman Pots the clock has to be distributed with great precision only over the small region of the Roman Pots, while the synchronization between the Roman Pots and the central detector will be within a bunch crossing of about 9 ns. Right now, for RHIC the reference for Beam Sync is supplied by the RHIC LLRF System, the jitter of this system is 200fs-ish, so sub-ps, integrated over something like a 1Hz-100kHz bandwidth. This clock will be used as basis for the t0 of the Rp and from the experience of LHC and NSLS-II this can be done to 5 ps. There is no reason to assume the "eRHIC-clock" based on the eRHIC LLRF System would be worth, especially as these signals are used to cog the beams.

Maintaining this performance as the clock is distributed across the RP detector will require inter-calibrating the reference time t0. The clock dispersion requirement for the ATLAS and CMS timing detectors will be of the order of 5 ps over a far larger detector area. Static (e.g. alignment, time-of-flight, cable delays) and dynamic (e.g. high-frequency jitter, noise) contributions to the timing calibration are being studied for LHC applications and such studies will be leveraged for the EIC application. In particular, for the most difficult case, i.e. the dynamic contributions, for which data statistics may be a problem to calibrate away fast effects, real-time calibration has been studied. This real-time calibration uses a technique based on the measurement of the mean of the time-of-arrival distribution (t0) over a certain period of time. At the LHC it was estimated that this value can be used to dynamically correct the cumulative time offset of each channel individually with a t0 precision in the order of few ps. Ultimately calibration constants will be computed online in the FELIX off-detector readout board and then applied offline at the event reconstruction phase.

1.2. Recommendation:

Proceed to full proposal, but the proponents are requested to:

- *Indicate the physics motivation for going to 10 ps timing resolution and motivate the pixel parameters such as pixel size through physics simulations;*

Please see earlier discussion why the timing resolution in the ballpark of 10 ps is needed. A detailed study of the detector requirements is part of the deliverable of this proposal and are therefore not yet provided.

- *Present a research plan for the sensor design to achieve a timing resolution of 10 picoseconds, including system aspects;*

The preliminary results of the first 4x4 AC-LGAD sensors fabricated at BNL already show a time jitter of few tens of ps, with no optimization. By optimizing the doping concentration of the gain layer we will control the gain, hence the time resolution. At BNL we have produced several batches of LGADs with different gains, up to about 80, with very good electrical and timing performance, and we have achieved good confidence in our fabrication process that will be applied to the next AC-LGAD batches that are already in production.

The optimization will not be limited to the achievement of the target goal of about 10 ps time resolution, but will also extend to ensuring stability, reliability, and overall optimal performance of the whole device. An optimization of the AC-LGAD design and fabrication technique is on-going to increase the break-down voltage and in turn ensure operational stability of the devices up to higher bias voltages (hence higher gains). As part of the planned optimization for this project, we also plan to make the *n*-resistive layer for the AC-coupling more resistive to achieve a more effective insulation among pads. The resistivity of the *n*-resistive layer need optimization to minimize cross-talk between pixels by changing the doping concentration depending on the target pixel pitch. This optimization is on-going and will be completed in the next months.

Critically for this project we need to optimize the inactive edges. The AC-LGAD produced at BNL so far have a conservative design with several protective guard rings that reduce the active area at the edges of the device. For an application of AC-LGAD in Roman Pots the size of the guard ring area will be reduced to maximize the active area. This optimization will be dedicated to and driven by the application of AC-LGADs to Roman Pots in the context of this proposal.

The final detector will include a TDC and the data will be read out by the combination of CARIBOU and FELIX readout boards, developed by the ATLAS collaboration with a major intellectual and technical contribution by BNL. The CARIBOU board receives the digital signal from the detector and converts it in an optical signal for the FELIX board. The FELIX board is a major part of the ATLAS DAQ system for HL-LHC, while CARIBOU has been successfully used in test beams at FNAL, CERN and PSI for reading out Pixel detectors for ATLAS, NASA and CLIC in conjunction with FELIX board.

In the context of this R&D project the sensors we will be read out by streaming the analog signals to off-detector electronics, thanks to the low occupancy and low-noise/self-triggering feature of the devices under study. For test-beams in Phase-2 of the project we will read out only a few channels using the CARIBOU+FELIX system together with a dedicated ADC to be designed by the electronics group at BNL. During the feasibility study in the 1st year of the project, for the readout of the AC-LGAD and 3D sensors we will use single and multi-channel fast-timing printed circuit boards (PCB) in use at BNL, designed for the ATLAS and CMS timing detectors by colleagues at SCIPP and by FNAL, respectively. More specifically, the single channel boards will allow prompt diagnostics of new sensors, while the 16-channel PCB developed will allow us to carry out detailed tests, for example of the charge sharing among neighboring pixels.

- *Elaborate on the results obtained with the current four-pixel AC-LGAD sensors;*

After fabrication, a few samples were diced out from the wafer and mounted on printed circuit boards (PCB). They have been read-out by fast transimpedance amplifiers (TA) (PCB developed by SCIPP, Santa Cruz), see Figure 2 below. Signals induced by either X-rays from ^{55}Fe or beta radiation from ^{90}Sr have been acquired by means of a 1 Ghz oscilloscope. As yet, AC-LGADs consisting of a single pad (about 1 mm x 1 mm), and consisting of 4, 9 or more pads (about 500 micron x 500 micron, 200 micron x 200 micron each or less) have been measured. Being the read-out electronics a single-channel TA, only one pad at a time can be measured, while the others are grounded. The *n*+ at the border has been kept either at ground (GND) or connected to a 1 MOhm resistor towards GND, to make the *n*+ and the *n*-resistive layer floating, similar to the situation of an AC-coupled silicon microstrip. Examples of waveforms acquired with the 4-pad AC-LGAD are shown in Figure 2 (*n*+ to 1 MOhm resistor to

ground, using a ^{90}Sr source). Despite the pad under measure sees a low resistance path toward ground (the other three pads are in fact at GND and are capacitively coupled to the *n*-resistive layer), the Johnson thermal noise induced by the interpad resistance is negligible and the total noise is similar to the noise of a standard LGAD.

In the wafer layout, we inserted an AC-LGAD with a layout compatible with the commercial read-out chip, and we plan to bump-bond such sensor to the chip in the near future.

With the 16-channel board designed and fabricated by colleagues at FNAL, we have tested the performance of 3x3 (9-pad) AC-LGAD devices featuring 200 micron x 200 micron pads, by reading out multiple channels at a time, for example the signal sharing between pixels. Figure 4 above shows the waveforms of adjacent and next-to-adjacent pixels using a beta beam form a ^{90}Sr source at BNL. A charge sharing of the order of 35% is visible between adjacent pixels and about 20% (or less) for the next-to-adjacent channels. This will be further reduced in the future by adjusting the resistivity of the *n*-resistive layer in the new batch of AC-LGAD that is currently in production.

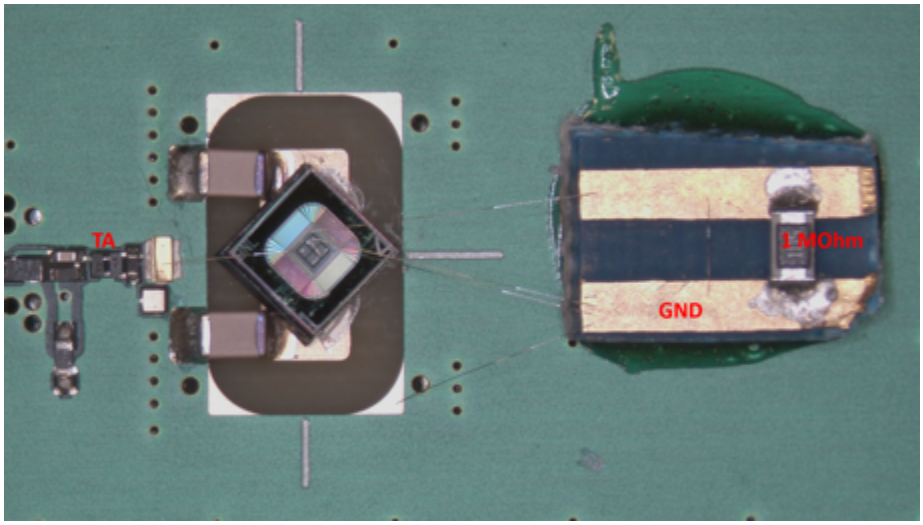

Figure 3: Test setup, showing the AC-LGAD test structure connected to the single channel TA, and its connection to GND or to 1 MOhm.

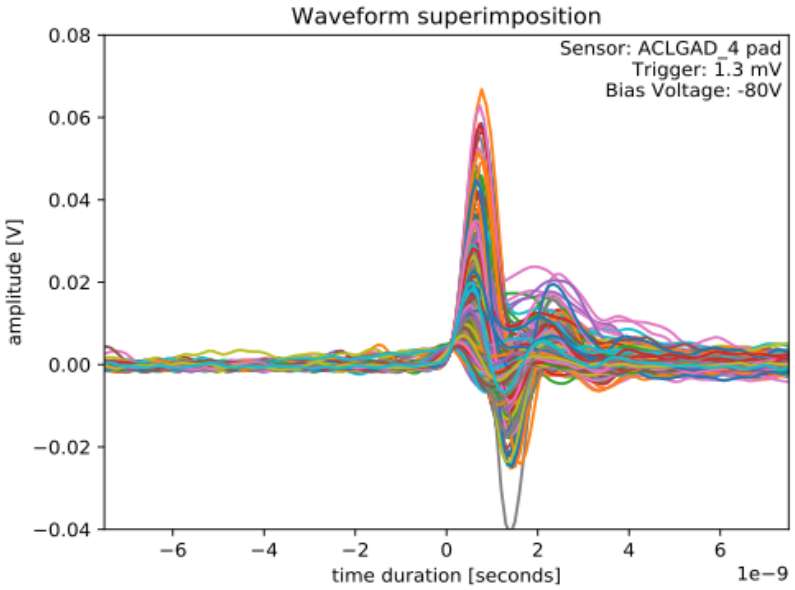

Figure 4: Waveforms as acquired from the scope, generated by beta radiation from ^{90}Sr impinging a 4-pad AC-LGAD.

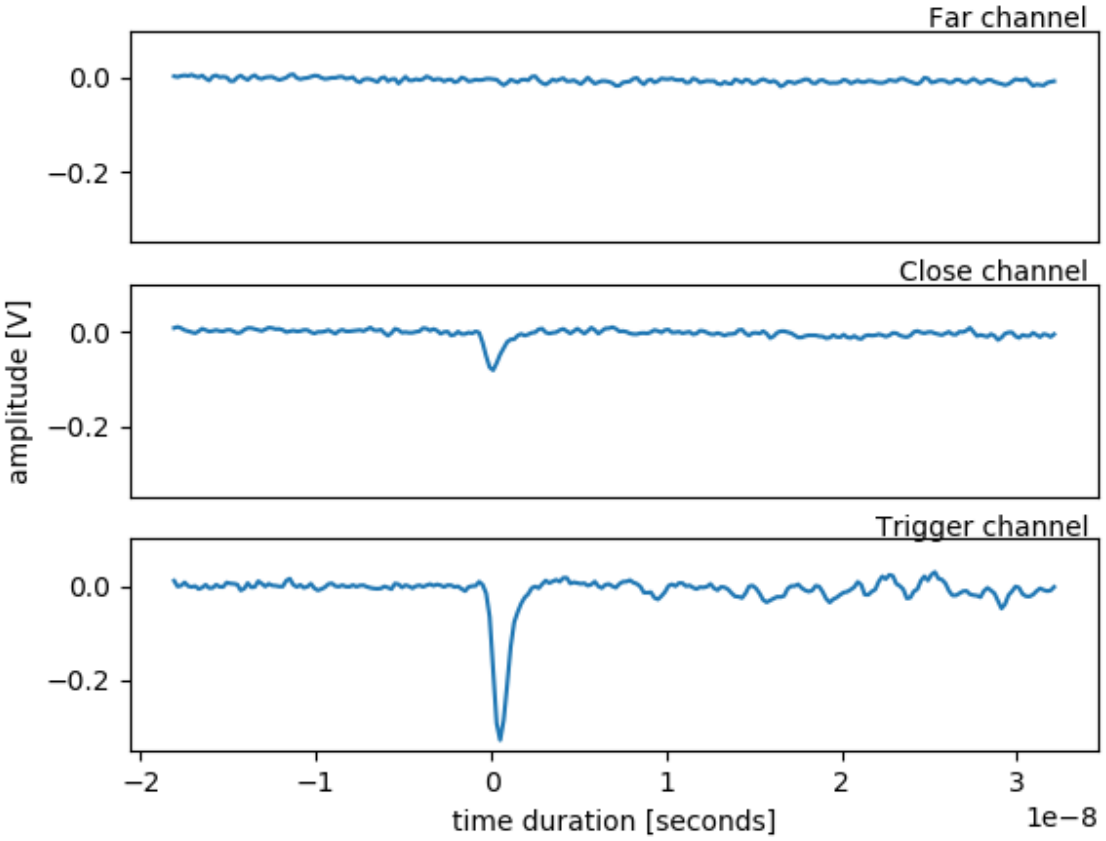

Figure 5: Waveforms as acquired from the scope, generated by beta radiation from ^{90}Sr impinging a 3x3 (9-pad) AC-LGAD, readout by a 16-channel board with trans-impedance amplifier. At the bottom we see the waveform from the channel that triggers the readout of all channels, in the middle we see the waveform from an adjacent channel, at the top the one from a next-to-adjacent channel.

- *Outline the resources required for phase-2 of the proposal that are expected to be supported by this program.*

In Phase-2 we plan to build a small-scale demonstrator of the detector with either (or both) AC-LGADs or 3D detectors and test it at RHIC in the STAR interaction region. For this demonstrator we will use the AC-LGADs with the design optimized according to Phase-1 studies, with the pixel pitch determined by the Phase-1 physics analysis and fabricated with larger pixel arrays to closely mimic the final design. We will stream out the data to off-detector electronics, which will comprise an ADC together with CARIBOU and FELIX readout boards.

For the Phase-2 part of the project we will ask for support for the design of the ADC board to be interfaced to CARIBOU, the readout system setup and installation in the test-beam, in addition to human resources for test-beam operations and data analysis. We expect a request of support for 0.20 FTE of an electronic engineer, 0.10 FTE for a technician, 0.20 FTE of a PostDoc, and 0.20 FTE of a student, in addition to approximately $15,000 for materials and consumables. We will keep leveraging contributed/in-kind BNL resources for the AC-LGAD design optimization, fabrication and testing, and contributed effort of BNL and SBU scientists.

2. Scientific Motivation

Quantum Chromodynamics (QCD), the theory of the strong interaction, is a cornerstone of the Standard Model of modern physics. It explains all nuclear matter as bound states of point-like fermions, known as quarks, and gauge bosons, known as gluons. The gluons bind not only quarks but also interact with themselves. Unlike with the more familiar atomic and molecular matter, the interactions and structures are inextricably mixed up, and the observed properties of nucleons and nuclei, such as mass and spin, emerge out of this complex system.

Deep-inelastic scattering (DIS), the basic process at the EIC, because of its unmatched precision, is the ideal tool to study the inner structure of nuclear matter. The distribution of partons inside nucleons and nuclei depends on the scale, Q^2, which specifies the resolution at which partons are resolved, and the momentum fraction, x, carried by the parton relative to the momentum of the nucleon. Both variables (x, Q^2) define the kinematics and regime probed in a DIS measurement and can be controlled event-by-event. **Figure 6** shows schematically how going from high x (~1) to small x (~$10^{-4\text{-}5}$) at a resolution scale Q^2 of a few GeV^2 reveals a more and more complicated structure of quarks and gluons inside the proton. The proton goes from a few-body regime with its structure dominated by the valence quarks to a many-body regime dominated by the quark-gluon dynamics responsible for hadron structure, to a collective regime dominated by gluons generated through QCD radiation and at last to the saturation regime where the parton densities are so large that the gluon radiation is balanced by gluon recombination leading to non-linear effects.

Understanding the observed properties of nucleons or nuclei, such as mass or spin, requires to be able to probe all regimes and the transition from one regime to the other and to explore how the observed properties emerge from the complex, strongly-interacting many-body systems of nuclear matter. The EIC with versatile beam energies and species and a broad range in x and Q^2 will be the right tool to unravel the QCD structures and dynamics of matter.

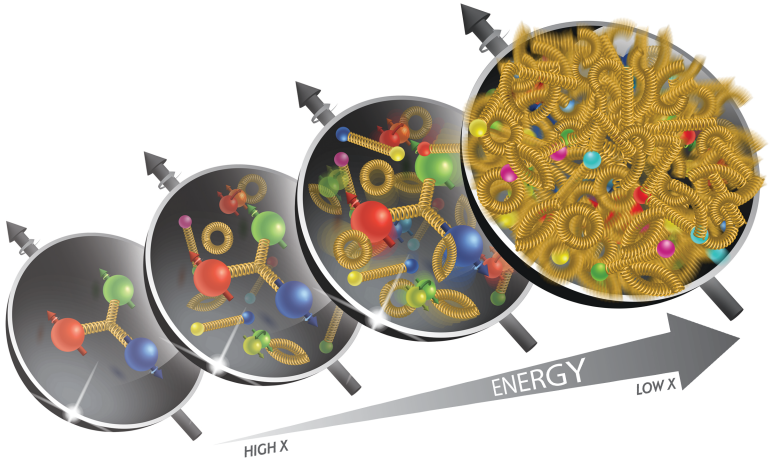

Figure 6: *The development of the internal quark and gluon structure of the proton going from high to low x. Decreasing x corresponds to increasing the center-of-mass energy.*

Till today the consolidated understanding of the nucleon structure is basically one-dimensional. In inclusive DIS, the nucleon appears as a bunch of fast-moving quarks, antiquarks and gluons, whose transverse positions and momenta are not resolved. EIC will open up the unique opportunity to go far beyond this one-dimensional picture of the nucleon. It will enable parton femtoscopy by imaging quarks and gluons in transverse position and momentum space for all kinematic regimes. Such "tomographic images" will provide insight into the QCD dynamics inside hadrons, such as the interplay between sea quarks and gluons and the role of pion degrees of freedom at large transverse distances.

1.3. Nucleons and Nuclei in Three Dimensions

As discussed above, inclusive DIS measurements provide us only with information about the longitudinal motion, *x*, of partons (see Figure 7) in a fast-moving nucleon, but no information about the transverse positions or momenta of partons can be obtained. Although a fast-moving nucleon is Lorentz-contracted, its transverse size is still about 1fm, which is the typical scale of non-perturbative interactions, where phenomena such as confinement occur.

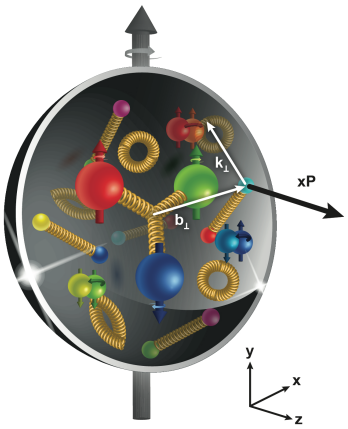

Figure 7: *Schematic view of a parton inside the proton with longitudinal momentum fraction x, transverse position b_T and transverse momentum k_T in the proton.*

This leads to fundamental questions such as:

- How are quarks spatially distributed inside the nucleon?
- How do they move in the transverse plane?
- Is there a correlation between orbital motion of quarks, their spin, and the spin of the nucleon?
- How can we access information on such spin-orbit correlations, and what will this tell us about the nucleon?

The above questions address two complementary aspects of the nucleon structure: the distribution of quarks and gluons in the transverse plane in momentum space and in coordinate space. We still lack quantitative answers to these questions, but in recent years we have obtained a much better idea on how to answer them due to recent theoretical progress [1]. Generalized Parton Distributions (GPDs) and Transverse Momentum Dependent parton distributions (TMDs) are the novel tools in QCD that allow us to study the inner structure in three dimensions.

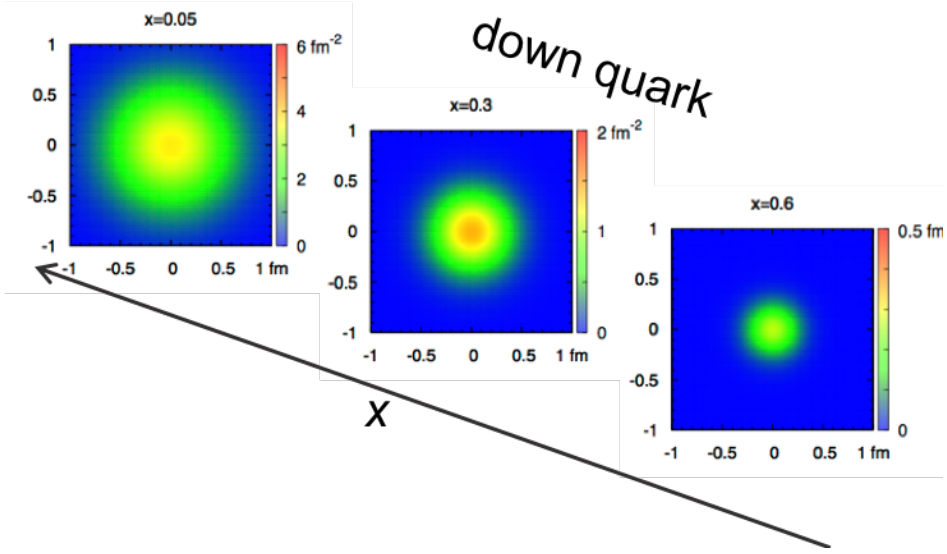

Figure 8*: Transverse position snapshots of a down quarks in an unpolarized nucleon for three values in x. The color coding of the three panels indicates the probability of finding the down quark.*

In addition to the longitudinal momentum fraction *x*, GPDs provide information about the transverse position b_T (see Figure 8). TMDs describe the inner structure in momentum space as a function of *x* and the transverse momentum k_T. One of the key goals of an EIC is to precisely image the momentum and spatial structure of quarks and gluons.

As in the case of the transverse momentum distribution of partons inside a hadron, we know little about what a hadron looks like in transverse spatial dimensions. Many of our expectations are solely based on models. In some cases, it is expected that at large-*x*, the quantum numbers of the hadrons come from the struck partons in the DIS measurement. As one goes to low-*x*, and gluon distribution begins to saturate, it's an interesting question of how gluons and sea quarks clump together in the hadron. It is now possible to measure the transverse spatial distributions experimentally. The study of the spatial distribution of quarks and gluons requires a special category of measurements, that of exclusive reactions. Examples are Deeply Virtual Compton Scattering (DVCS) [2] and Deeply Virtual Vector Meson (DVVM) production. In these, the proton remains intact after the electron has scattered off, and either a photon or a vector meson is produced.

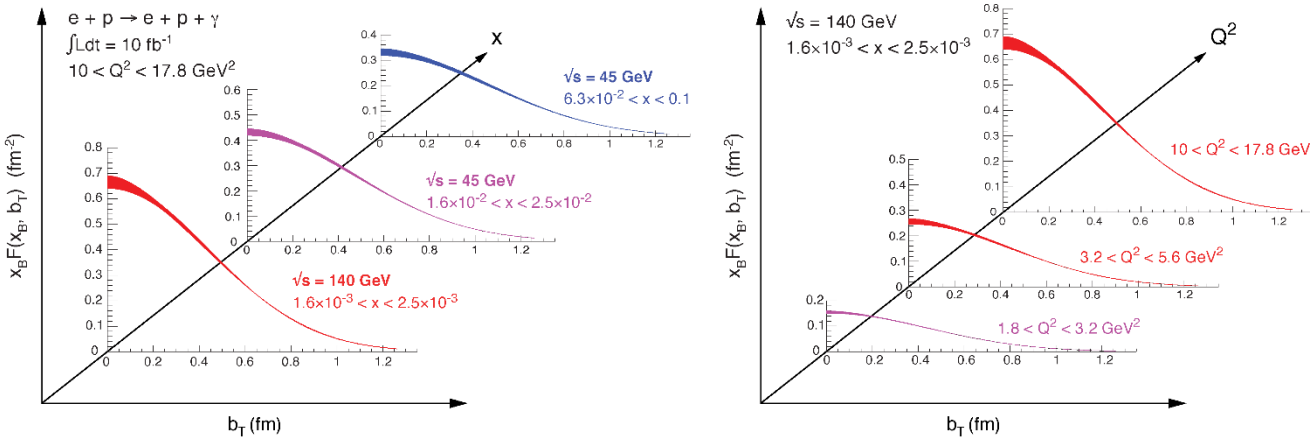

Figure 9: *The projected precision of the transverse spatial distribution of partons obtained from the Fourier transform of the measurement of unpolarized DVCS cross section as a function of |t| at the EIC for a targeted luminosity of 10 fb-1 at each center-of-mass energy. Impact parameter, b_T, is the distance from the center of the proton. Left: the evolution in x at a fixed Q^2 ($10 < Q^2 < 17.8$ GeV^2). Right: the evolution in Q^2 at a fixed x ($1.6\text{x}10^{-3} < x < 2.5\text{x}10^{-3}$). The red and blue bands indicate extraction of spatial distribution only with high and low center-of-mass energies, respectively, while the purple band is accessible at both.*

Exclusivity demands that all final state products are detected. This includes the scattered electron, the produced photon or vector meson, and the scattered proton. The spatial distribution of quarks and gluons in these experiments is extracted from the Fourier transform of the differential cross section with respect to the momentum transfer, *t*, between the incoming and the scattered proton. GPDs are not only interesting because they encode the spatial distributions, but also because the second moment of particular sets of quark and gluon GPDs will give us information about total angular momentum of quarks and gluons in the proton [3]. It is anticipated that measurements made for protons in the range $0.04 < t < 1.6$ GeV^2 (corresponding to $0.2 < p_T < 1.3$ GeV) will enable maps of parton distributions all the way down to 0.1 fm [2,4]. Such exclusive measurements performed on nuclei will enable us to gain a deeper understanding of the transverse quark and gluon distributions within. Figure 9 shows the precision with which an EIC will provide transverse spatial distribution for quarks [4]. The red and blue bands are reachable only with high or low energy collider operations, respectively, while the purple band is reachable by both. The measurements were simulated using an integrated sample of 10 fb^{-1}. The uncertainties shown in this plot only account for statistics and experimental systematics.

1.4. Scientific Requirements

Exclusive processes require a careful design of the detector and the IR in the outgoing proton/nucleus beam direction. Contrary to exclusive electron-proton events, for electron-nucleus collisions it is not possible to tag the outgoing intact scattered nucleus. Therefore, another technique needs to be realized to ensure exclusivity. One can require a "rapidity gap" in the detector, meaning that there is a region in the detector from the hadron beam towards the center of the detector in which there is no activity from the hadronic final state. The efficiency for detecting exclusive events and their purity therefore depends strongly on the rapidity coverage of the detector. Simulations have shown that a rapidity coverage of -2 to 4 is required to have both detection efficiency and a purity greater than 90% for exclusive e+A events, assuming a cross section ratio of Exclusive-to-DIS events of 10:90 as measured at HERA. Therefore, no collider equipment can be installed inside the main detector volume and/or extend beyond 1.5° not to compromise the efficiency and purity of exclusive events that are detected through the rapidity-gap method. In general, for exclusive reactions, one wishes to map the four-momentum transfer, or Mandelstam variable t ($= p_T^2$ of the scattered proton) of the hadronic system, and then obtain an image of the spatial partonic structure of the proton by a Fourier transform of the (un)polarized cross section as function of t. Figure 10 (left) shows what fraction of the beam momentum ($X_L = p'_L/p_{Beam}$) is carried by these scattered protons as measured by ZEUS at HERA [5] and on the right the correlation between the proton scattering angle and its momentum. This illustrates that the remaining baryonic states go in the very forward proton-beam direction. Even at a proton energy of 50 GeV, the proton scattering angles only range to about 25 mrad. At proton energies of 250 GeV, this number is further reduced by a factor of five. In all cases, the scattering angles are small. The main detector reaches down to a rapidity -4 to 4, corresponding to 35 mrad from the beam line. Therefore, these protons are not seen in the main detector and need a different technique to be detected, i.e. Roman Pots. Roman Pots (RPs) are moveable detectors used in high energy and nuclear physics collider experiments. Several detector stations are in general positioned several meters away from the interaction point. They are critical to detect the collision products that are scattered under very small angles with respect to the incoming beam direction. The basic technology for RPs are silicon detectors, which need to be positioned as close as possible to the core of the beam in order to maximize the acceptance of the forward scattered particles. The acceptance strongly depends on the exact interaction region design and the details of the design of the Roman Pots.

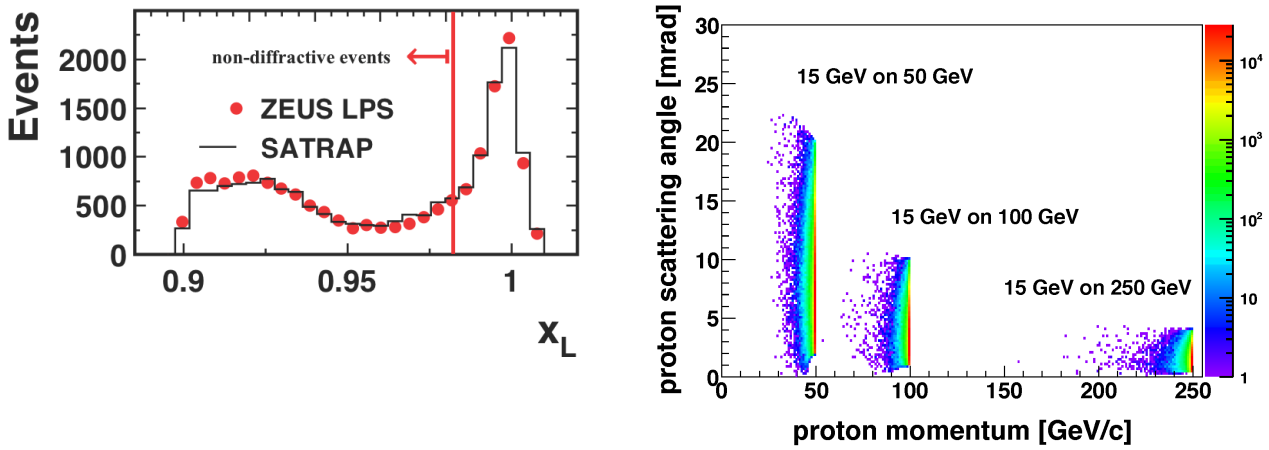

Figure 10: *Left: Fraction of the beam momentum carried by the scattered protons as measured by ZEUS at HERA. Right: The scattered proton momentum vs. scattering angle in the laboratory frame for DVCS events with different beam energy combinations. The following cuts have been applied: 1 GeV^2 < Q^2 < 100 GeV^2, 0.01 < y < 0.85, 10^{-5} < x < 0.5 and 0.01 GeV^2 < t < 1 GeV^2. The angle of the recoiling hadronic system is directly and inversely correlated with the proton energy. It thus decreases with increasing proton energy.*

Figure 11 (top) shows the cross section of exclusive real photon production (DVCS: ep → e'p'γ) as function of t. The red dots represent the measurements and their statistical precision as obtained at eRHIC for √s = 141 GeV and an integrated luminosity of 10 fb^{-1} for 0.03 GeV^2 < |t| < 1.6 GeV^2 corresponding to an acceptance in

p_T of 0.18 GeV/c < p_T < 1.3 GeV/c, which is the nominal requirement from the EIC White Paper. The blue curves represent an exponential fit to the measured points for different regions in *t* with the width of the band representing the uncertainty of the fit. The different rows show the result for different acceptances in p_T of the scattered protons. The lower row shows the impact parameter dependent PDF obtained from a Fourier transform of the cross-section measurement with different p_T acceptances. The bands represent the parametric errors in the fit and the uncertainty from different extrapolations to the regions of unmeasured (very low and very high) p_T of the scattered protons. Based on these studies and the EIC White Paper, protons with 0.18 GeV/c < p_T < 1.3 GeV/c need to be transported through the IR.

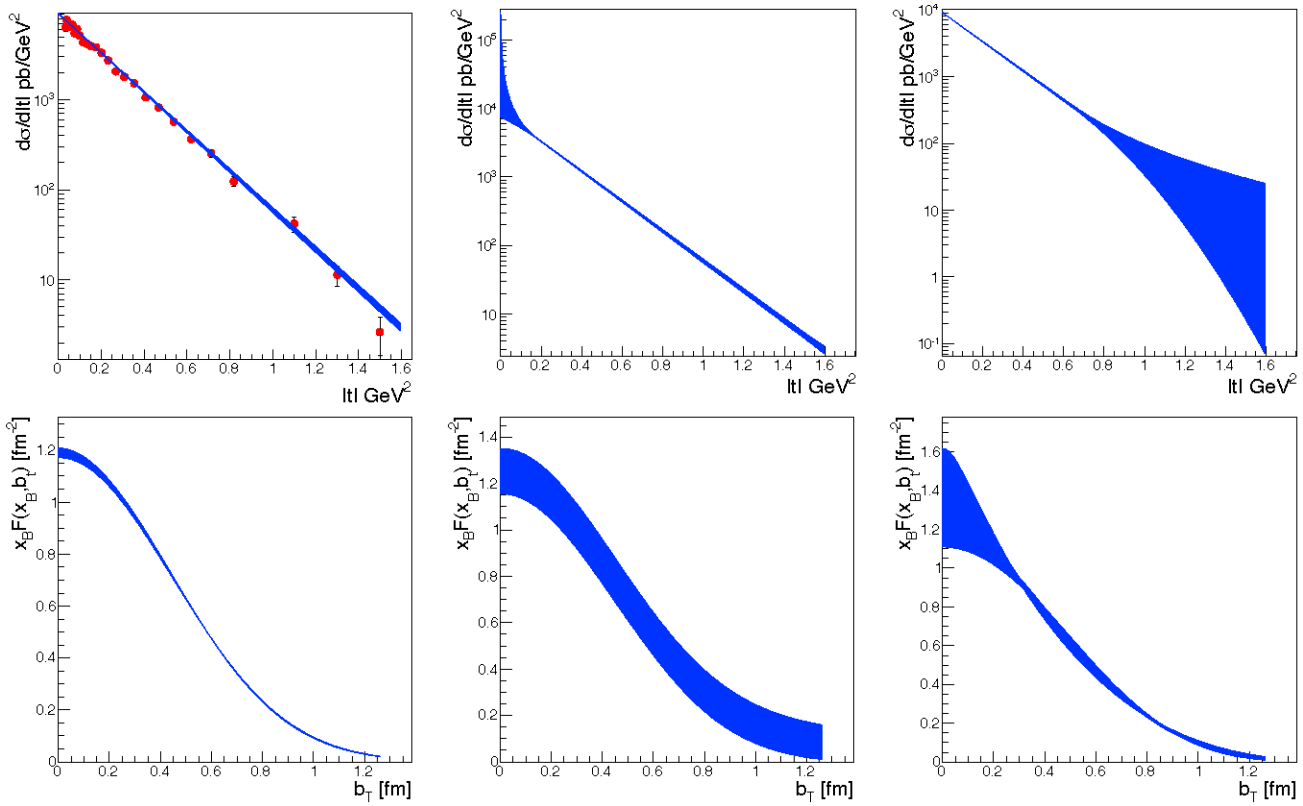

Figure 11: *Top: The cross section as function of t. The red dots represent the measurements and their statistical precision as obtained at eRHIC for √s = 141 GeV and an integrated luminosity of 10 fb^{-1}. The blue curves represent an exponential fit to the measured points for different regions in t, with the width of the band representing the uncertainty of the fit. The different rows show the result for different acceptances in p_T of the scattered protons. Bottom: The impact parameter dependent PDF obtained from a Fourier transform of the measured cross section with different p_T acceptances. The bands represent the parametric errors in the fit and the uncertainty from different extrapolations to the regions of unmeasured (very low and very high) p_T of the scattered protons. Left: 0.18 GeV/c < p_T < 1.3 GeV/c, 0.03 GeV^2 < |t| < 1.6 GeV^2; Middle: 0.44 GeV/c < p_T < 1.3 GeV/c; Right: 0.18 GeV/c < p_T < 0.8 GeV/c.*

1.5. Realization of the Scientific Requirements in the Interaction Region

As emphasized strongly earlier the detection of forward-going scattered protons from exclusive reactions as well as of neutrons from the breakup of heavy ions in incoherent and non-diffractive reactions is particularly challenging. Extreme care needs to be taken to transport protons with 0.2 GeV/c < p_T < 1.3 GeV/c through the IR (see Figure 12) such that they can be detected as soon as they can be separated from the core of the beam. To achieve this p_T coverage over a wide range of center-of-mass energies a multi-prong approach is required. Protons with scattering angles up to 5 mrad are detected in the Roman Pots, while the range from 7 to 20 mrad is covered

by the B0 large-acceptance spectrometer. The main detector in general starts seeing secondary particles above ~30 mrad (η ~ 4) and bending power of the 3T solenoid is sufficient for momentum measurement above ~50 mrad (η ~3.5 or so).

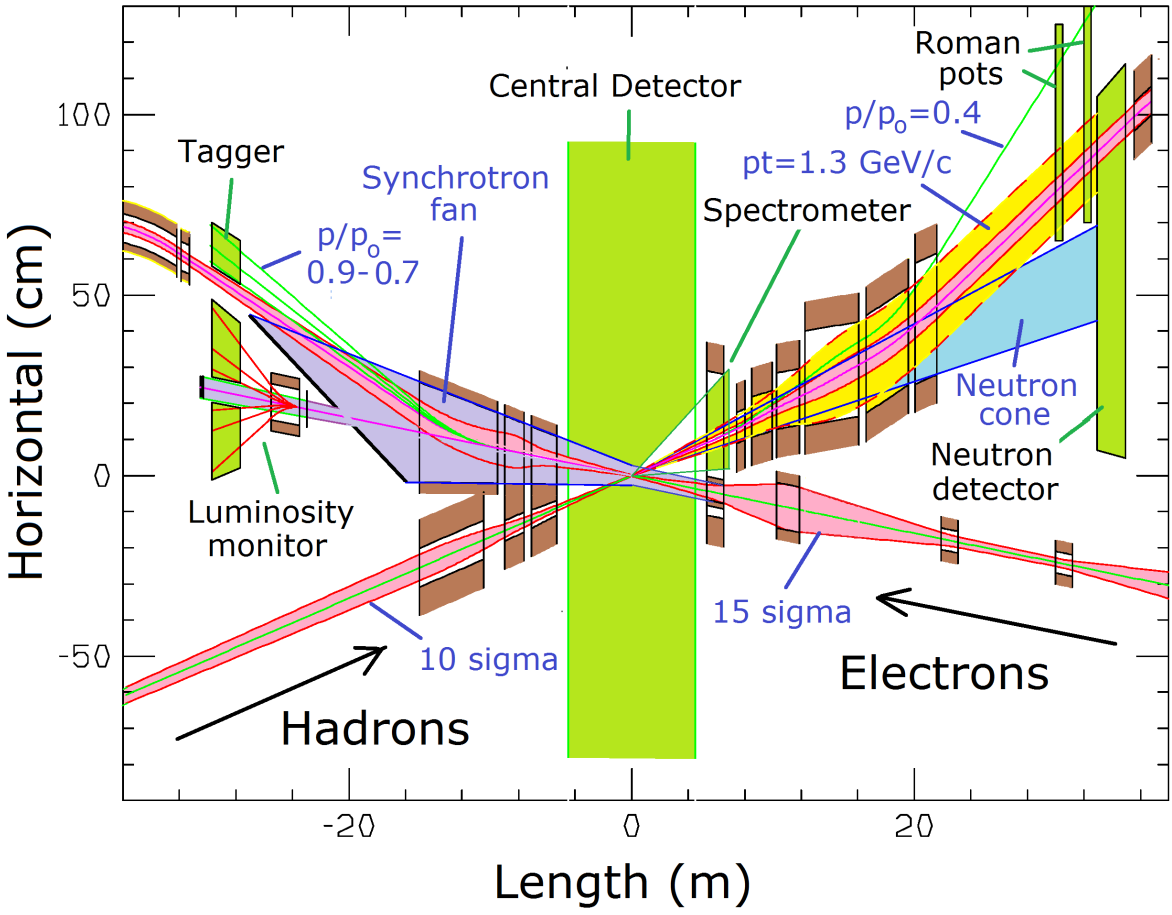

Figure 12: *Schematic layout of the eRHIC IR.*

In the current IR design, Roman Pots stations are placed at ~35 m downstream of the IP. There are several effects influencing the low p_T acceptance. We have been following the general rule of thumb that the distance between the edge of the Roman Pot silicon sensors and the beam orbit should be 10 σ in X and Y. The physical size of the separation $\sigma_{x,y} = \sqrt{(\beta_{x,y}\epsilon_n)/\gamma}$ is driven by the normalized beam emittance ϵ_n and the β-functions $\beta_{x,y}$ at the location of the Roman Pots. The acceptance at large p_T is mainly constrained by the magnet apertures.

Figure 10 (right) illustrate the need for a multi-prong detector approach to provide the full p_T acceptance over a wide range of hadron beam energies as it can be expected that multiple detectors are needed to cover the full range in scattering angles at different energies. For E_p = 41 GeV the limiting factor in acceptance at high p_T is the inner dimension of the vacuum chamber and the magnet apertures. At E_p = 100 GeV one in general has full acceptance in p_T but there can exists some "grey" (transition) area separating the forward scattered proton acceptances in the B0 spectrometer and the Roman Pots. For E_p = 275 GeV the acceptance is mainly limited at low p_T by the beam envelope size at the Roman Pot location and consequently the 10 σ separation cut. Therefore, it is of paramount importance that the active area of the silicon sensor is as close as possible to its physical edge. For that reason, we propose here an evolution of the standard design of silicon detectors used in Roman Pots, in a way they can closely surround the beam spot by design of the optimal shape of the silicon, reducing the dead area to a minimum.

The p_T resolution of these forward scattered particles is of equal importance as their acceptance. There are several effects that can influence the momentum resolution and need to be mitigated:

- The spread in the beam energy, which normally has a width (RMS) of ~ 10^{-4}.
- The finite width of the vertex distribution at the IP adds uncertainty in the angle determination. This uncertainty can in principle be eliminated by determining the vertex of the event through other tracks in the event being registered in the main detector and benefit from the excellent vertex definition by the μ-vertex detector. But for exclusive reactions, especially the DVCS there are very small numbers of tracks or only one the scattered lepton. At low Q^2 the scattered lepton has a very shallow angle and therefore the vertex resolution is not very precise.
- The angular divergence $\sigma_\theta = \sqrt{\epsilon_n/(\beta^*\gamma)}$ of the beam, which directly leads to a smearing of the scattering angle.
- The hadron bunch "rotation" at the IP due to the crab cavities (see
- Figure **13**) is 25 mrad for eRHIC and 50 mrad for JLEIC. Crabbing implies a transverse momentum kick $p_x(z)$ to the particle bunch, with the kicking strength proportional to the longitudinal position z of particles in the bunch. Therefore, the IP particles at the "head" of the bunch will have a slightly different orientation and/or transverse offset compared to the ones in the "tail" of the bunch, which leads to additional smearing of the apparent scattering angle. The z-vertex determination of the event provided by the main tracker as well as high-resolution timing of the Roman Pot silicon sensors (of an order of ~10 ps or so) should be able to mitigate this effect to a large extent, but more studies are needed, which are part of this proposal.

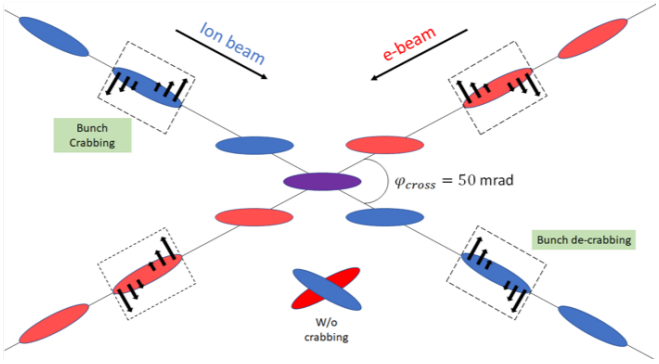

Figure 13: *Schematic to explain the concept of crabbing.*

We are planning to use EicRoot as a software suite to perform the simulation studies, since it has most part of the required functionality implemented and tested already:

- Essential part of the Interaction Region vacuum system STEP file import
- Beam line element location and magnetic field description (MAD-X files), as well as the apertures
- Main eRHIC general purpose detector description, including central tracker and vertex detectors for DVCS electron track reconstruction, as well as the electromagnetic calorimeter for DVCS photon kinematics reconstruction
- Kalman filter based scattered electron track fitting and vertex determination algorithms
- Monte-Carlo event import for several DIS generators, including DVCS MILOU ASCII files
- Crossing angle definition, as well as part of the effective "primary interaction spot" description (an expected convolution of the proton and electron beam bunch profiles at the IP)

The existing software requires further development though, which will be an integral part of the deliverables of this proposal:

- Vacuum system CAD file import tools need to be refined and made more versatile in order to allow for a more precise IR geometry description

- MAD-X file based transport matrix calculation from the RP location to the IP needs to be automated, as well as the 10 σ stay clear cut setting at the RP
- A consistent description of proton and electron bunch geometry (both transverse and longitudinal profiles), as well as the angular spread for given emittances and optics tuning are missing
- Consistent crab cavity effect simulation in GEANT may require dynamic electric field parameterization
- Time-of-flight part of the code, in particular z-vertex reconstruction based on the timing measured at the RP location, has to be developed
- Kinematic fitting, which is a distinguishing feature of the exclusive event reconstruction, needs to be incorporated in order to establish ultimate requirements on the silicon detector spatial and timing resolutions

3. Development of an edgeless 4D detector: AC-LGAD

Silicon detectors are ideal for applications in Roman Pots thanks to their radiation hardness and fine pixelation that can provide fine spatial resolution tracking devices. Recent developments in silicon technologies have shown that they can also be designed to achieve fast time resolution, ideal in particle physics experiments for vertex finding. Studies of fast-timing detectors have attracted widespread interest in the scientific community around the world in relation to the development of the next generation of collider experiments and imaging techniques for a variety of applications. Silicon-based particle sensors that combine fast-timing and radiation-hardness properties are a rapidly developing research area, thanks to their applications in timing and tracking systems for the upgraded ATLAS [6] and CMS [7] experiments at the CERN Large Hadron Collider (LHC) for the High Luminosity phase (HL-LHC) [8,9], which is expected to begin in 2026. One of the selected technologies for such detectors, that can deliver the required timing performance of a few tens of ps, is a silicon pad with internal amplification: the so-called Low-Gain Avalanche Diode (LGAD) [10,11].

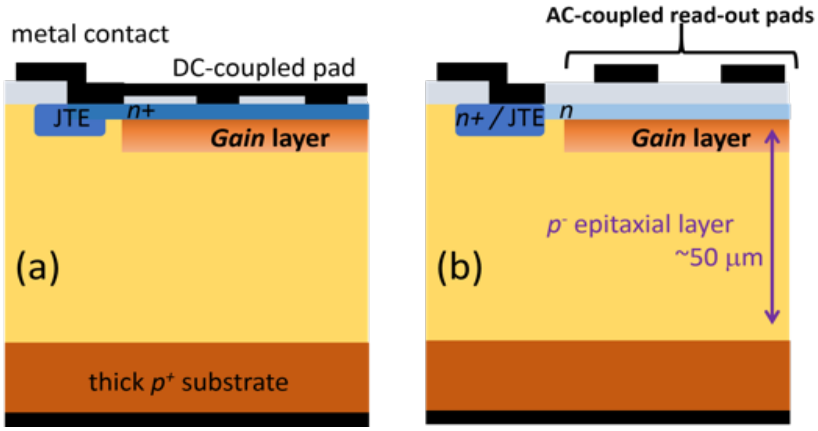

Figure 14: *(a) sketch of a standard LGAD, with a pad defined by an n+ over a gain p⁻ layer, and contacted by a metal pad; (b) an AC-LGAD, where the n+ is replaced by an n resistive layer, and the metal pads are patterned over a dielectric.*

Attaining time resolution in the order of few tens of picoseconds or less requires a combination of high signal-to-noise ratio and short rise time. LGADs exhibit moderate gain values (typically 10 to 50), achieved with high electric fields within the semiconductor material, which enable drifting electrons to create impact ionization. LGADs have recently attracted attention since their radiation hardness up to $3x10^{15}$ neutrons/cm^2 and timing resolution of a few tens of picoseconds have been demonstrated [12], however a condition for a uniform multiplication across the full area of the device is for such area to be far larger than the thickness of the substrate. For example, in the High Granularity Timing Detector (HGTD) of ATLAS [6] at the HL-LHC, LGAD pads are about 1.3 mm x 1.3 mm and thickness of 50 um. Therefore, if on one hand timing is very good, on the other hand spatial resolution is poor.

An innovative approach to provide at once good timing and spatial resolution is to exploit the AC-coupled LGAD option [13]. In this device, finely spaced metal electrodes are AC-coupled to the silicon bulk and provide the needed granularity, as seen in Figure 14.

BNL is active in the development of standard LGADs [14] and is now investigating this new and novel approach of AC-LGADs. In the silicon fabrication facility in Instrumentation Division we have designed and fabricated 4 wafers of AC-LGADs. As yet, these consisting of a single pad (about 1 mm x 1 mm), of 4 (about 500 mm x 500 mm each or less) have been measured in a dedicated silicon characterization laboratory at BNL. Examples of waveforms, acquired with the 4-pad AC-LGAD exposed to a beta beam from ^{90}Sr, are shown in Figure 15, and calculating the time resolution term associated to the sensor noise jitter as $\sigma/(dS/dt)$, where σ is the sensor noise and dS/dt the slope of the signal S as a function of time t, we estimate a time resolution of the order of few tens of ps for this sensor. Other performance studies based on radioactive sources show that the total noise of individual pads is similar to the noise of a standard LGAD. In the plans is to read-out many channels in parallel.

Optimizations of the design and fabrication technique are ongoing, for example we will tune the operational voltage, the gain value and the insulation among pixels.

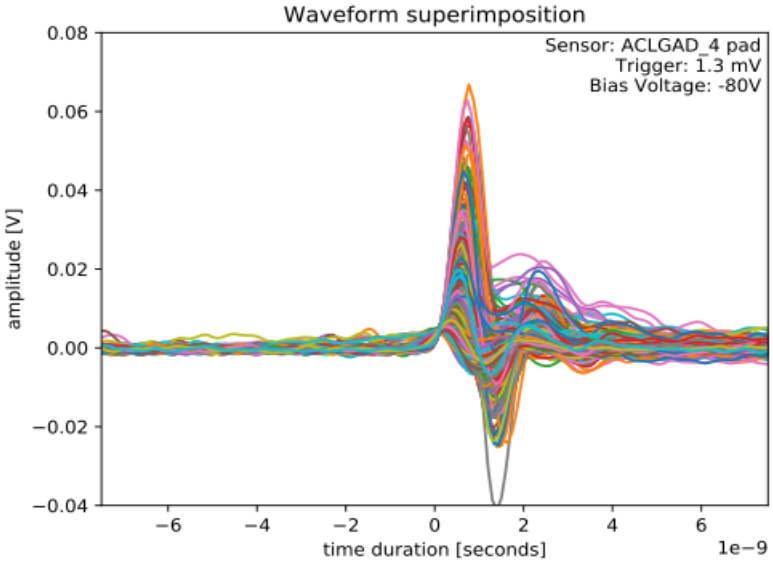

Figure 15: *Waveforms as acquired from the scope, generated by beta radiation from ^{90}Sr impinging a 4-pad AC-LGAD fabricated at BNL.*

In the wafers we also inserted AC-LGAD structures that are pixelated with the layout and pixel pitch (55 um x 55 um) compatible with commercial readout chips. This highly pixelated structure will be the basis for the detector demonstrator that we aim at designing, fabricating and testing for this proposal. In the first year we will focus on the optimization of the design and fabrication of highly-pixelated AC-LGADs that match the requirements defined by physics performance studies: most notably the pixel multiplicity and pitch, time resolution, and last but not least the size of the non-sensitive area (edges), which is critical for their applications in a Roman Pot. As visible from Figure 16, current AC-LGADs have wide edges, due to the current design that includes several protective guard rings, therefore dedicated studies will be carried out in the first year of this project to develop AC-LGAD with reduced edge size, that meets the requirements set by physics studies. A way to reduce the extension of the termination area is to implement a trench just at the active area border, creating thus an “active edge” structure [15]. The trench can be etched in silicon by plasma methods (e.g., dry etchings or Deep Reactive Ion Etchings or DRIE). Trenching also provides protection against breakdown. The DRIE technique is already in use for the etching of columnar electrodes in silicon, see below. For this project we will leverage resources available in the Physics Department and Instrumentation Division for the characterization of fast-time silicon sensors. The optimization of the AC-LGAD design for this project will benefit from the AC-LGAD R&D on-going at BNL for applications in HEP, quantum information and imaging.

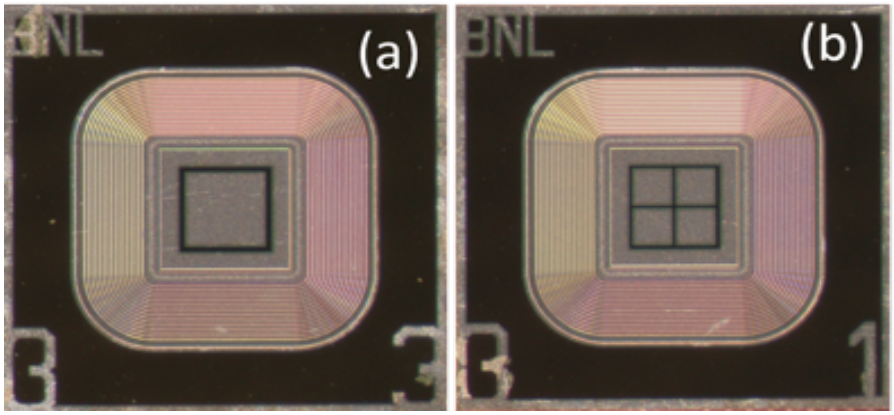

Figure 16: Pictures of some of the test structures of AC-LGADs inserted in a dedicated wafer fabricated at BNL. (a) Single pad; (b) 2x2 pad array.

Alternative detector technology: 3D sensors

In parallel with the development of a 4D detector based on AC-LGAD technology that BNL is pioneering, we plan to study an alternative technology, called 3D silicon detectors, and compare the performance of these two technologies. In 3D silicon detectors, proposed in 1995 by S. Parker [16], the electrodes are processed inside the detector bulk instead of being implanted on the wafer's surface, i.e. the electrodes penetrate vertically throughout the sensor's bulk [17]. In this configuration the electric field is parallel to the wafer's surface. The inter-electrode distance can be made very short, largely reducing collection time without affecting the signal amplitude. The shorter distance implies lower trapping probability after irradiation, in addition to faster response time, and lower depletion voltage, which also leads to lower power dissipation. Figure 17 illustrates the different charge collection mechanism between a planar sensor and a 3D sensor.

The 3D-based detectors have been demonstrated to be highly tolerant to radiation and have been operating in the newly installed lowest layer of the ATLAS pixel detector, the ATLAS Insertable B-Layer (IBL) since 2014 [18]. Most importantly for this project 3D detectors feature small edges by design. These sensors are currently produced for LHC applications by FBK (Trento, Italy) and CNM (Barcelona, Spain). The 3D detectors have the advantage over AC-LGADs of being an established technology that is radiation hard and generally with small edges. However, we need to carefully assess whether their time resolution and the edge size meet the requirements of Roman Pots in this project. Also, their production costs are higher than for AC-LGADs, given their more complex fabrication process. The DRIE etching technique, as presented above, will be used to investigate both technologies: the 3D pixel sensors and the active edge as termination in a planar AC-LGAD sensor.

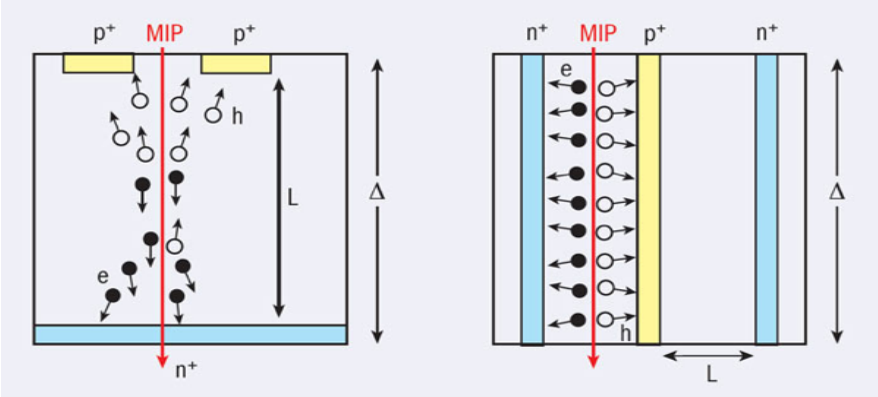

Figure 17: *(left) A planar detector where the depletion region between the two electrodes, L, grows vertically as close as possible to the substrate thickness, Δ. (right) In 3D sensors the electrode distance, L, and the substrate thickness, Δ, are decoupled because the depletion region grows laterally between electrodes whose separation is far smaller than the substrate thickness; the full depletion voltage, which depends on L and grows with the increase of radiation-induced space charge, can be reduced drastically [19].*

4. Proposed program of work and deliverables

We propose to split this proposal in several phases. Each of the phases strongly depends on the outcome of the prior phase. In this write-up we discuss in detail the 1st phase of the project, which is to be completed in one year.

Simulations in Phase-1:

We propose to utilize the existing EicRoot software framework, which has an up-to-date implementation of the eRHIC IR and is interfaced with the different DIS Monte Carlo generators to simulate different physics

scenarios relying on Roman Pots to detect forward scattered particles. We will develop a tracking code, which propagates the particles produced at small scattering angles through the beam line magnets from the IP to the Roman Pots. With this code the achievable angular and momentum resolution will be studied as function of the timing resolution of the silicon sensors to unfold the effect of the transverse momentum kick $p_x(z)$ to the particle bunch because of the crabbing of the beam.

In addition, we will determine the achievable z-vertex resolution combining the tracking information of the scattered electron and the forward scattered particles. The simulations will integrate all the accelerator effects, i.e. beam angular divergence and energy spread, to obtain a realistic assessment of the importance of the size of the non-active region at the edge of the sensors. The program will also include a study of the optimal geometrical shape of the Si-Sensor to achieve the best acceptance for forward scattered particles. All these simulations will be performed taking into account specific geometrical layouts and constraints of both detector technologies under consideration (AC-LGAD and 3D detectors) to determine the optimal solution for the EIC detector Roman Pots.

Through the EICUG Interaction Region Working Group we will collaborate with the experts at Jefferson Lab and provide them with our simulation software tools to carry out studies on the impact of the higher bunch frequency and larger crossing angle on the requirements and choice of the detector technology.

Sensor development in Phase-1:

The current BNL production of AC-LGADs is not optimized for a Roman Pot application: the number of guard rings, and in turn the size of the edge, is large, the pixelation geometry targets applications in HEP and photon science. Furthermore, the performance, e.g. timing and charge sharing among pixels etc. is still under careful assessment. In this project we will leverage the on-going AC-LGAD R&D for HEP and photon science and focus on the design and fabrication of AC-LGADs prototypes that target applications in Roman Pots, i.e. with a small size of the sensor edges and with the timing performance and geometry layout that meet the requirements set by the physics simulation studies.

More specifically, in the 1st phase we foresee 3 batches of few 4-inch wafers being designed and fabricated at BNL:

- 1st batch: design of few AC-LGADs devices with small numbers of guard rings to establish minimum edge size possible.
- 2nd batch: design of small-edge AC-LGADs with different geometrical layouts, e.g. pixel multiplicity and pitch, in the range of requirements set by preliminary simulation studies.
- 3rd batch: optimized AC-LGAD design that best matches final requirements set by physics studies with the goal to study ultimate detector performance.

The performance of the 3rd batch of AC-LGADs will be compared with the performance, e.g. electrical, timing and spatial resolution, of the established technology of 3D detectors provided by SBU/Manchester. For performance studies we will leverage equipment and resources available in Physics Department and Instrumentation Division for fast-timing detector characterization.

Planned activities in Phase-2:

The 2nd phase of the project in year 2 will focus on building a detector demonstrator of the chosen technology, AC-LGAD or 3D, and test the sensor performance with beam in the STAR experiment. The integration of a detector demonstrator into the STAR Roman Pots will be part of phase 2 of the proposal and will include the design of the on/off-detector electronics for readout. We will leverage expertise and resources in Physics Department and Instrumentation Division for the development of the readout electronics.

Milestones:

1. Set of requirements on the needed timing resolution of the Si-sensors, geometrical layout and the maximum allowed non-active region of the Si-Sensors such that the acceptance of the forward scattered particles is not impacted.
2. Three batches of AC-LGADs with different designs for optimization studies
3. Comparison of performance of optimized AC-LGAD and 3D sensors.
4. Assessment of the pro's and con's for scientific requirements as well as for integration into the accelerator, cost, schedule and operations and of the 2 possible technologies for Roman Pots at an EIC.

Deliverables:

1. Set of physics performance goals for Roman Pots at EIC.
2. Set of requirements for detectors for application in Roman Pots at an EIC.
3. Set of specifications of AC-LGADs and 3D silicon sensors that meet Roman Pot requirements for application at EIC.

5. Proposed Budget and Labor

A budget of **$35,000** is requested for the 1st phase of the proposal. The costs and labor are detailed below and are summarized in Table 3and Figure 18.

4.1 Labor

- **$ 20,000** for 0.10 FTE of a scientist (G. Giacomini) for sensor design and fabrication in the clean room of the Instrumentation Division at BNL.

4.2 M&S

- For the silicon R&D part of the project we request funds for fabrication of AC-LGADs with optimized design, specifically to meet the physics requirements of Roman Pots: **$10,000** which include masks and 3 silicon production batches.

4.3 Travel

- For the study of 3D sensors and comparison with AC-LGADs we request **$5,000** for an international travel and subsistence for a student to visit BNL and join the local group on laboratory measurements for 2 months.

Costed Item	Direct Cost [$]
Labor	20,000
M&S	10,000
Travel	5,000
Total	**35,000**

Table 3: Breakdown of budget request for Phase-1 of the project.

4.4 External Funding

For the simulation part of the proposal we utilize funds from the approved 3-year program development project "eRHIC: from Virtual to Real" of E.C. Aschenauer to support the labor needed to perform all the simulations. For the silicon R&D part of this project we will leverage resources from A. Tricoli's Early Career Award

and LDRD for the development of fast-timing silicon detectors (LGADs) for HEP and photon science, respectively.

4.5 Contributed Labor

Simulations to determine Scientific Requirements

- 0.15 FTE E.C. Aschenauer to supervise the simulations to determine the scientific requirements.
- 0.4 FTE of a PostDoc in the group of E.C. Aschenauer to perform the needed simulations.
- 0.25 FTE of a PhD student (W. Chang) in the group of E.C. Aschenauer to perform the needed simulations

Sensor Development and Testing:

- 0.10 FTE of A. Tricoli in Physics Department to supervise students and Post Docs at BNL.
- 0.15 FTE of a BNL PostDoc and 0.10 FTE of a job-shopper for laboratory measurements.
- 1.00 FTE of a BNL summer student.
- 0.10 FTE of Professor C. Da Via at SBU/Manchester to supervise a student on 3D sensor analysis.

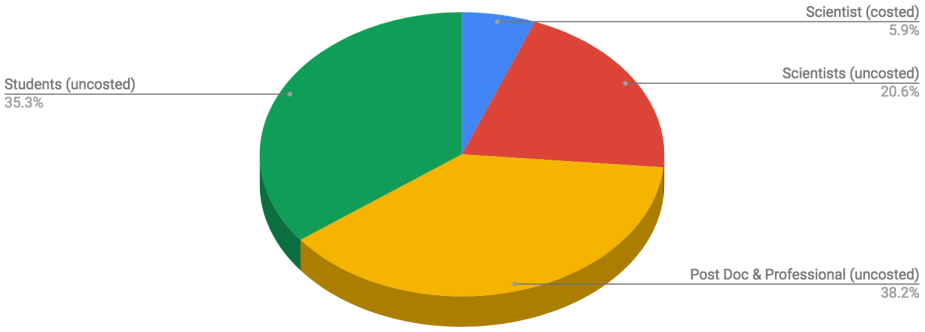

Figure 18: Labor contribution to 1st Phase of the project. It includes costed and contributed labor.

References:

[1] The 3-D Structure of the Nucleon, M. Anselmino, et al. Eur. Phys. J. A (2016) 52. 164.
[2] E.C. Aschenauer, S. Fazio, K. Kumericki, and D. Mueller, JHEP09(2013)093.
[3] X.-D. Ji, "Gauge invariant decomposition of nucleon spin," Phys. Rev. Lett., vol. 78, pp. 610–613, 1997.
[4] E. C. Aschenauer, S. Fazio, J. H. Lee, H. Mantysaari, B. S. Page, B. Schenke, T. Ullrich, R. Venugopalan, and P. Zurita, "The Electron-Ion Collider: Assessing the Energy Dependence of Key Measurements," arXiv:1708.01527, 2017.
[5] S. Chekanov et al., "Leading proton production in deep inelastic scattering at HERA," JHEP, vol. 06, p. 074, 2009
[6] ATLAS Collaboration, Technical Proposal: A High-Granularity Timing Detector for the ATLAS Phase-II Upgrade, Tech. Rep. CERN-LHCC-2018-023.LHCC-P-012, CERN, Geneva (Jun 2018). URL: http://cds.cern.ch/record/2623663
[7] CMS Collaboration, TECHNICAL PROPOSAL FOR A MIP TIMING DE-TECTOR IN THE CMS EXPERIMENT PHASE 2 UPGRADE, Tech. Rep.CERN-LHCC-2017-027. LHCC-P-009, CERN, Geneva (Dec 2017).URL: https://cds.cern.ch/record/2296612
[8] L. Rossi, O. Bruning, High Luminosity Large Hadron Collider: A description for the European Strategy Preparatory Group, Geneva (Aug 2012). URL: https://cds.cern.ch/record/1471000
[9] I. Bejar Alonso, L. Rossi, HiLumi LHC Technical Design Report: Deliverable:D1.10 (Nov 2015). URL: https://cds.cern.ch/record/2069130

[10] H. F-W Sadrozinski et al., "4D tracking with ultra-fast silicon detectors," 2018 Rep. Prog. Phys. 81 026101, https://doi.org/10.1088/1361-6633/aa94d3.
[11] G. Pellegrini et al., "Technology developments and first measurements of LowGain Avalanche Detectors (LGAD) for high energy physics applications," Nuclear Instruments and Methods in Physics Research A765 (2014) 12–16, http://dx.doi.org/10.1016/j.nima.2014.06 .008.
[12] N. Cartiglia et al., "Beam test results of a 16 ps timing system based on ultra-fast silicon detectors," Nuclear Instruments and Methods in Physics Research A 850 (2017)83–88, http://dx.doi.org/10.1016/j.nima.2017.01.021.
[13] M. Mandurino, "Resistive AC-Coupling: a new readout paradigm in 4D tracking with Ultra-Fast Silicon Detectors," 13th "Trento" Workshop – Munich, 19-21 February 2018.
[14] G. Giacomini et al., "Development of a technology for the fabrication of Low-Gain Avalanche Detectors at BNL," NIMA(2019), https://doi.org/10.1016/j.nima.2019.04.073.
[15] M. Povoli, et al.: "Design and testing of an innovative slim-edge termination for silicon radiation detectors", 2013 JINST 8 C11022 (IWORID 2013)
[16] I. Parker, C. J. Kenney, J. Segal, *"3D - A proposed new architecture for solid-state radiation detectors"*, Nucl. Instrum. Methods Phys. Res. A, vol. A395, pp. 328-343, 1997.
[17] C. Da Via, *"3D sensors and micro-fabricated detector systems"*, Nucl. Instr. And Meth. In Phys. Res. A Volume 765, 21 November 2014, Pages 151–154, and references therein.
[18] CERN Courier, May 31, 2012.
[19] The ATLAS Collaboration, *"ATLAS Phase-II Upgrade Scoping Document"*, CERN-LHCC-2010-0013, URL: https://cds.cern.ch/record/1291633